New Advances in Automated Urban Modelling from Airborne Laser Scanning Data

Short running title: Automated Urban Modelling from Aerial LiDAR

Abstract: Traditionally, urban models in many applications such as urban planning, disaster management, and computer games only require visual accuracy. However, more recently, updating urban infrastructure combined with the rise of mega-cities (i.e. those with populations over ten million) has motivated researchers and users to utilize city-scale models for engineering purposes (e.g. tracking pollution monitoring, optimizing solar panel placement), which necessitate high geometric accuracy. Currently, a major bottleneck lies in the cost of generating accurate, geo-spatially referenced models. This paper presents the evolution of some of the efforts to automatically produce such models. Specifically, recent advances in airborne laser scanning can rapidly acquire accurate, spatial data for large geographic areas in hours, but due to the size of the data sets, coupled with difficulties of capturing and portraying complex structures, many post-processing issues have only recently been addressed to a level sufficient to begin to facilitate automation, especially of building surface reconstruction. Automation is a critical step for further processing and utilization of airborne laser scanned data for engineering-based, urban modeling. This paper presents recent development of the methods for building detection and extraction, with an emphasis on patents and other contributions related to automated processing of airborne laser scanning data.

Key Words: Aerial/airborne laser scanning, three-dimensional (3D) spatial data, urban modeling, automated/automatic building detection, gaming, LiDAR (light detection and ranging)

INTRODUCTION

There is an increasing need for large-scale three-dimensional (3D) geometric models of urban areas for e.g. urban planners and civil engineers. These can include such seemingly disparate applications as predictive noise and pollution models or disaster mitigation. In the event of sudden infrastructure changes, such applications require accurate geometric models, and in post-disaster scenarios evaluating existing structures, models must be quickly generated. A major impediment to this has been the labor-intensiveness of such efforts. Recent breakthroughs in airborne laser scanning [also known as airborne Light Detection and Ranging (LiDAR)] flight path planning that emphasize building façade data capture has greatly facilitated the potential for rapid auto-generation of such models [1]. This paper presents the evolution of automated urban model construction, with an emphasis on airborne laser scanning data processing.

MATERIAL AND METHODS

Increasingly, large-scale computing efforts are being applied to urban planning and disaster management [2,3]. These applications range from optimizing single-incident fire department responses to predicting and mitigating regional flooding effects [4,5]. Many of these efforts have relied upon geographic information systems (GISs). Typically, governmental agencies maintain GIS basemaps of their jurisdiction. The majority of these basemaps are limited to two-dimensional (2D) representations, with 3D functionalities being limited to a highly narrow set of applications (e.g. to assess the impact of natural disasters [5,6]). In coming decades, as population and urbanization expands, threats to the quality of life issues (e.g. preservation of natural resources, green spaces, air quality, historic structures, and quiet zones) will continue to intensify. As such, better computer modeling capabilities related to these topics will be needed. Visualizing the large datasets involved in such city-scale surveys poses significant challenges (e.g. [7]).

One major issue has been data collection. An airborne laser scanner (ALS) generates large collections of points, called point clouds. The unstructured nature of these point clouds makes them unsuitable for effective direct visualization and engineering purposes. To enhance their usability, further processing is needed. The tasks of visualizing laser scanning data can be divided into two areas: (1) surface reconstruction from point clouds (e.g. [8]), which is a noise-sensitive procedure, the success of which is largely dependent on the quality of the sampled points; and (2) visualization of reconstructed surfaces, where efficient scene representations and caching methods must be employed in order to allow modern rendering engines to cope with the enormous data-sets involved. Visualization is crucial to understanding and analyzing large datasets and is, therefore, a critical issue in large-scale urban planning.

Visual System Population

The visual population of GISs with urban structures has been implemented in a variety of ways, and difficulties arise when populating these and virtual cities (only some of which are GIS-based). The typical result is a graphically enhanced system that provides 2D images applied to various surfaces within a system. One approach is to combine a simple 3D model with detailed, real-world texture maps. Jepson et al. [9] did this by overlaying a GIS-based terrain and aerial photographs to position the final models with respect to the road network. A sophisticated version of this was used in the Virtual Dublin project, which used 3D Studio Max to model the surface structure of the buildings [10]. For that, an initial street map from the original computer aided design (CAD) was required, textures of each building façade were created from suitable resolution digital photographs, and aerial photographs of the city were added to texture the building roofs. Other approaches are described below.

Visual and Geometric Modeling from Imagery

Early attempts at modeling from imagery employed a photogrammetric method to reconstruct scene geometry from photographs, which combines both geometry-based and image-based modeling techniques [11]. The reconstructed models were then textured in a view-dependent fashion, with the texture manually selected from the original photographs projecting onto the models. The view-dependent texture mapping consists of multiple views of a scene that better simulate geometric details on a basic model. Similarly, in the MIT City Scanning Project extensive research was conducted towards automated models of structures for urban simulation [12]. A novel device was developed to automatically acquire building pictures, and then several algorithms were developed to perform 3D reconstruction both feature-based and region-based. Façade structure and texture were auto-extracted from calibrated pose imagery [13]. This method used sets of images from known positions, which were then correlated to extract vertical façade features. Wang et al. [14] extended this technique with the recovery of microstructure features, such as recessed windows, by incorporating multiple images of the same structure from different angles. These techniques relied on calibrated cameras being used from known global positioning system (GPS) positions. Similarly, Lee et al. [15] developed a method for automatically texturing the rough wireframe models of building models that had previously been generated from aerial photographs and ground-based, uncalibrated camera images.

Visual and Geometric Modeling from Procedural Generation

Since the visualization of a city needs to be comprised of site-specific, real-world data, and details. Images can be generated using various approaches by concentrating resources on well-known areas and central landmarks. Artificially generated data can be used to complete more distant geographic areas, with sufficient variety and detail without loss of visual credibility. Parish and Müller [16] employed such an approach using an L-system grammar following topography and population density maps (which may be real or artificially generated) as the basis for road network generation. Their system then divided the blocks between roads into allotments and used another L-system to create building models. A semi-procedural approach was used to texture details on the buildings by using pictures of actual buildings projected onto the surfaces of each building. Based on template-based patterns, a virtual traffic network for a given region was generated with a special focus on modeling large urban structures from 2D input images [17].

To create a virtual Manhattan, building generation was guided by user input related to building type and supplemented by manual building insertion [18]. Alternatively, shape grammars can be exploited to generate building models, which allow rapid development of detailed, varying building models, according to rules derived from the real world as demonstrated by Wonka et al. [19]. In contrast, Laycock and Day [20] generated 3D building models by extruding building footprints from GIS landline map data with building heights calculated directly from the laser scanning data.

Virtual City Examples

A sampling of available virtual cities shows a wide variety of the end users and technological orientations, from strictly manual constructions to grammar based modeling, and visual, auditory and haptic response feedback [21,22]. High-end visualization solutions are often developed for the gaming community, which rely on generating realistic scenarios of urban areas, as a part of their game play. The modeling of London for the game "The Getaway" [23] was constructed by manual data acquisition and application of acquired textures for façades similar to that employed in the Virtual Dublin project [10]. In all of these cases, what remains a limitation for their transformation beyond gaming

into something capable of engineering applications is that the information in the models is immutable. Arguably, remote sensing in the form of airborne laser scanning holds the potential to overcome this shortcoming.

AIRBORNE LASER SCANNING DATA

ALS has gained enormous popularity over the past decades due to its ability to rapidly acquire large amounts of accurate geo-spatially referenced data. Yet, because of data processing limitations, applications have generally been restricted to Digital Terrain Models (DTM) and Digital Elevation Maps (DEM). More recent efforts to auto-detect man-made objects (especially buildings) have encountered a number of difficulties from a large number of false-positives to the reliance on external (and often unavailable) data for pre-analysis and data segmentation.

Laser scanner output is a large collection of point samples on objects in a scene. Often, the purpose of such scans is to quickly and accurately create digital city models. For the majority of applications in digital city models, it is not sufficient to represent buildings with point samples. The main reason for this is that the points have no topological information (i.e. how the points are connected is unknown). For visualization and analysis purposes, working with surfaces is a superior approach. Surfaces are often represented in a piece-wise, linear pattern using meshes of triangles or quadrilaterals containing the critical topological information. However, going from point samples to surfaces is not trivial. Although most digital city models aim only to retain information about man-made structures, such as buildings and monuments, the ALS scanner will collect all objects within its line-of-sight. Therefore, the purpose of the segmentation is to identify which points belong to man-made structures and which do not. As regards to vertical surfaces, such as building walls, they do not tend to occur naturally in urban environments; if detectable, these can hamper surface extraction efforts. However, due to the large number of points present in current data sets, manual techniques for detecting building outlines are not economically feasible at a city-scale. Thus, automatic building outline detection is an important step in producing surface models of cities. Building outlines also provide some of the topological information required, since data points not within building outlines are not included. Once surfaces have been constructed, enhanced visualization and advanced modeling can be applied. There have been many attempts to achieve this. Rudimentary versions of some of these techniques are implemented in commercial ALS data processing software packages as described below.

AUTOMATED STRUCTURE DETECTION FROM ALS DATA

The following subsections briefly describe the various techniques that have been used for building outline extraction from ALS data. Note that hybrid variations of these techniques are common, however, success is always dependent on the most accurate data source. Thus, if one data source is much less accurate than the other, a hybrid approach makes little sense. Some approaches rely on 2D ground plans to identify building outlines. Unfortunately, ground plans are often unavailable or out of date, especially in a post-disaster scenario.

To assist in visualizing some of the concepts, ALS data of a study area located in central Dublin city, Ireland are used. The data were collected in 2007 using FLI-MAP 2 system with a scan rate of 150 scan lines per second and a pulse rate of 150,000 per second. Therefore, 1,000 pulses were emitted for each scan line and a total of 370,154 scan lines were acquired. The system operated at a scan angle of 60 degrees with an angular spacing of 60/100 degrees between pulses. The quoted accuracy of the FLI-MAP 2 system is 8 cm in the horizontal plane and 5 cm in the vertical direction, including both laser range and navigational errors [24]. As the data acquisition is emphasized to collect sufficient data points of vertical surfaces for 3D modeling, a fight path was designed as close to 45 degrees as possible to as many streets as possible [1]. The flying altitude over urban areas was chosen to be as low as possible and varied between 380 to 480 m, with an average value of around 400 m. Further, the widest possible scan angle for the ALS system of 60 degrees was used [24]. The study area of about 1 km^2 contains 205 blocks of buildings and some vegetation and was captured from 44 flight strips with 2,823 flight path points recorded with approximately 225 million points giving a point density of 225 points/m^2. As an overwhelming majority of surfaces in the study area are solid, in the form of streets and buildings, and a vast majority of points are first echoes, although secondary echoes are presented as a small portion of the points [24].

1.1 Aerial Photographs

Commonly, a digital camera is used along with the laser scanner during flyovers to capture color information. A number of photographs are taken during the flyover, and these can be rectified and merged to form a so-called orthophoto.

The orthophoto can be thought of as a "top-down" view, much like a traditional map. Using the information in this map, building outlines can sometimes be automatically identified. An example of a so-called false color orthophoto is shown in Fig. 1. A false color orthophoto is created by using the color values of the highest point within the pixel as the pixel color; a pixel is the most basic component of a digital image. Each pixel is a small square region in the image plane. Digital images are composed of a grid of pixels that represent the image data at different locations. From the outlined procedure, false color orthophotos can be created, which are conceptually identical to ordinary orthophotos.

In order to rectify and merge aerial photographs into an orthophoto, the underlying geometry must be known. The paradox here is that orthophotos are commonly used to determine geometry, and hence an estimated geometry must be employed during the creation of the orthophoto. Further, per definition, a perfect "top-down" view contains no explicit information about vertical surfaces. This means that implicit characteristics of such surfaces are the only way of identifying them. Such characteristics depend not only on the nature of the surfaces, but also on the surroundings of these surfaces, where exactly the characteristics are sought. Vosselman and Dijkman [25] outline a manifestation of this approach. Additionally, edges of building roofs can also be extracted based on colour aerial images by conventional edge detectors, e.g. using a Canny operator [26,27]. In contrast to pixel-based approaches above, an object-based approach, so-called eCognition, has also been used to extract the building outlines from aerial images [28]. Basic concepts of that method are that building blocks of object-oriented classifications are contiguous, homogenous, image segments. Image objects are generated by consideration of three parameters including a scale parameter (which determines the maximal heterogeneity value of the objects), homogeneity in color, and shape [28]. Users must determine threshold values for these parameters to suit with certain objects, in which the scale parameter can only be found empirically [29].

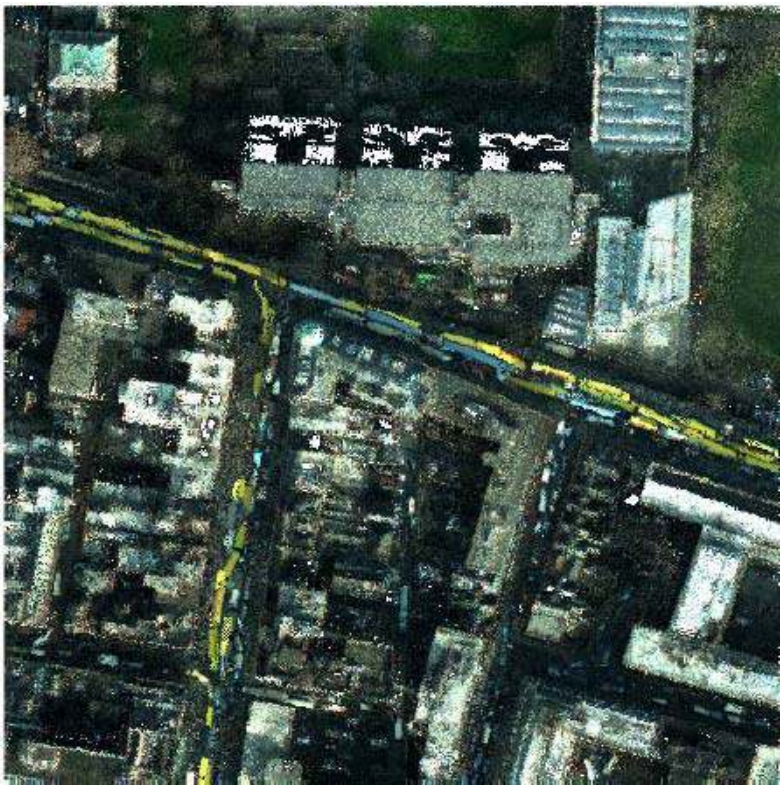

Fig. 1. By letting pixel values be the color value of the highest point in each pixel, a false color orthophoto can unintentionally be generated. Detecting building outlines from such an image is challenging. In this case, the thin rectangles lined end to end are bus roofs. Herein the pixel size represents an area of *0.25* m^2, and the image dimensions are *500* by *500* pixels.

Height Thresholding

Similar to the previous approach, height thresholding also relies on the construction of a "top-down" view of the scene. In this case, a digital image is constructed, where the height values of the pixels correspond to the height of the highest

point sample in each pixel (Fig. 2). An example of such an image is shown in Fig. 3. The simplest approach is to classify the pixels in the image according to their height. This can be done by comparing the height values to some threshold values. A more sophisticated approach assumes that height differences between neighboring pixels indicate walls. However, building walls are not the only manifestation of where height differences occur. Hence, in urban settings many outlines will be found, of which only the small subsets are building outlines. An example of a height threshold image is shown in Fig. 4. For this reason, when relying upon a single parameter, then height difference magnitudes must be compared to a threshold value and height differences smaller than this value are rejected as false outlines.

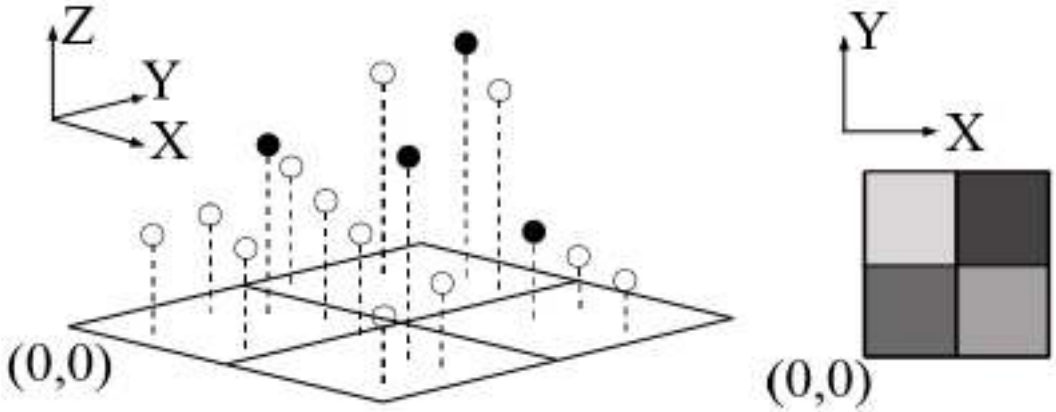

Fig. 2. Only the highest point in each pixel (blue points) determines the assigned depth image value (right). The larger the z-value of the highest point within the pixel, the brighter the pixel value will be. In this approach, much information is ignored (all red points) and subsequently not represented in the depth image.

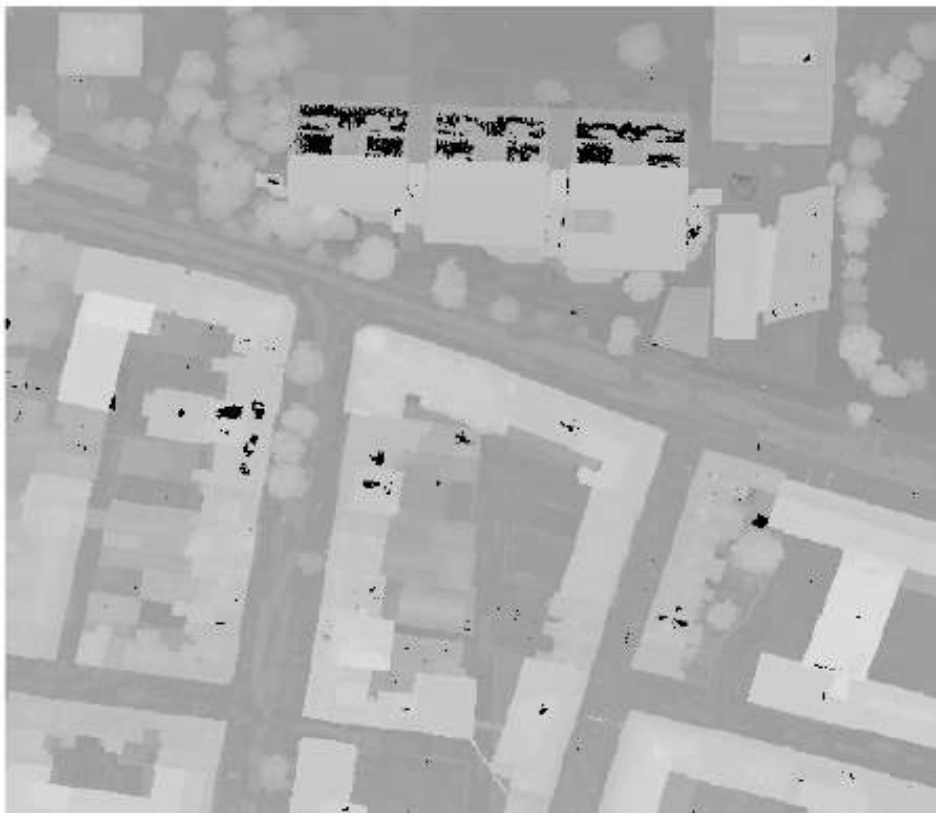

Fig. 3. An elevation image
(Created by mapping ALS point data to an image. Brighter pixels correspond to higher elevation points, and black pix-

els have no point samples in them, which identify that the scanner failed to detect the reflected laser pulse. Herein, the pixel size represents an area of *0.25* m^2, and the image dimensions are *500* by *500* pixels).

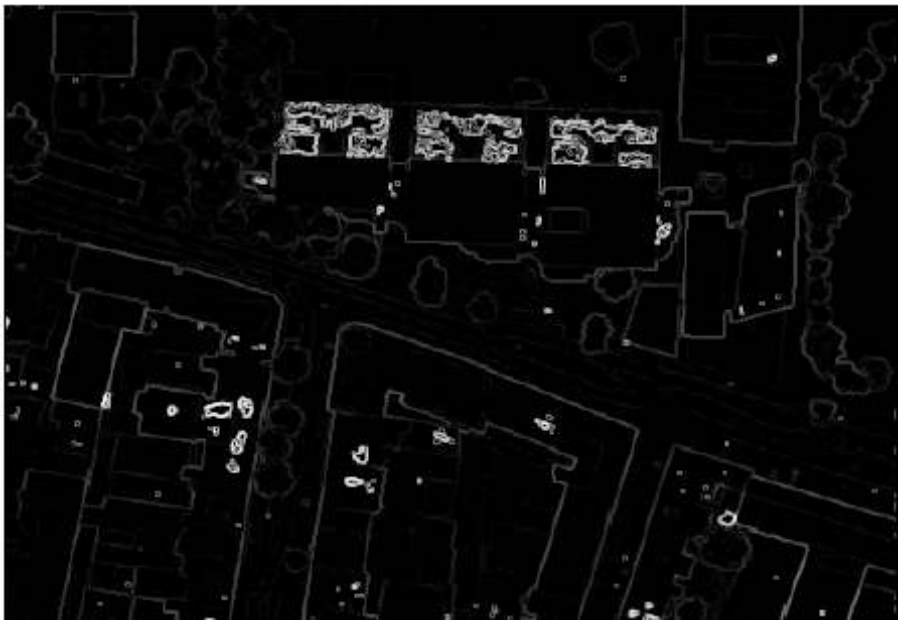

Fig. 4. Derived building outlines by using height threshold.
[After applying a height difference filter with a *5*m threshold, picking out building outlines remains difficult because of the large number of edges present. Also, some pixels have no points mapped to them, falsely indicating an edge – seen as bright spots (near the image's top and scattered in the middle). Herein the pixel size represents an area of *0.25* m^2, and the image dimensions are *500* by *500* pixels].

A single threshold value used for an entire scene offers little flexibility in terms of accurately processing different building sizes (e.g. low rise versus high rise) and types (e.g. residential versus commercial). Using threshold values is a tedious approach of segmentation, as it requires a lot of guessing and testing before a good value is found, and in many cases, no single threshold value will give a perfect (or even very good) segmentation. An example of such a scene is shown in Fig. 5.

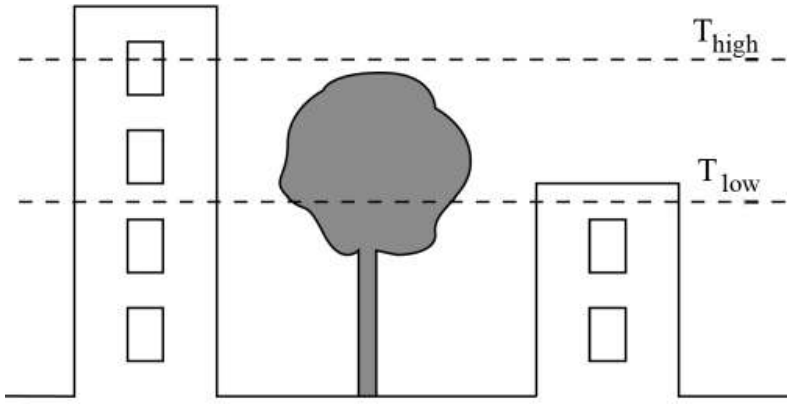

Fig. 5. The scene illustrates the difficulty of a single threshold. If an arbitrarily low threshold (T_{low}) is chosen, points on the tree crown will exceed the threshold. If an arbitrarily high threshold (T_{high}) is chosen, points on the lower building on the right will fail the threshold. For this scene, it is impossible to choose a threshold that both identifies the buildings and discards the tree.

If everything higher than a selected 5m threshold is classified as part of a building, then double-decker buses, billboards, tower cranes, and large trees will all be improperly included. Selecting a higher threshold value would unintentionally exclude single-story buildings. An example of using height differencing is shown in Fig. 4. Intensities in this image are proportional to the magnitude of the height difference at each pixel. The image shown contains false edges due to missing data (bright spots) and non-building outlines (e.g. from vegetation or vehicles in the streets). Distinguishing building outlines from other outlines in this image is difficult. For further use, a threshold must be applied, in order to remove false edges and non-building outlines. Choosing a suitable threshold value is problematic in this case, because the false edges have higher intensities than the building outlines, and the non-building outlines have lower intensities than the building outlines. This leads to a situation similar to that depicted in Fig. 5, where it is impossible to choose a single, threshold value that fully satisfies.

Orientation Thresholding

An alternative is applying a segmentation technique known as region growing for orientation thresholding. In this approach, a seed pixel containing a vertical surface is identified and becomes the initial seed pixel. The orientation of the surface at the seed pixel is compared to the orientations of the surfaces in surrounding pixels. If the difference in orientation between the seed pixel and its neighbors is smaller than some threshold, the neighbors become seed points in the next iteration. This continues until all pixels have been visited and evaluated. This can be a bit circular in nature, if the orientation of the initial seed pixel is not inherently known. Additionally, region-growing methods require threshold values in order to determine if neighboring surfaces belong to the same region. As mentioned above, it is difficult to find a threshold value that performs well for an entire scene.

In three dimensions, surface orientations are described by normal vectors (i.e. vectors perpendicular to the surface). However, where the underlying dataset is a point cloud, as for example from laser scanning, this means that the surface needs to be detected first before the normal can be computed accurately. Consequently, using orientations for automated building extraction is circular in nature. In addition, region-growing methods require threshold values in order to determine if neighboring surfaces belong to the same region.

Problems associated with these approaches

The above-described techniques assume that the data are sampled regularly across a planar grid. Because the scanner sweeps across the flight path during the scanning process, the data are in fact not sampled regularly; this is illustrated in Fig. 6. The main argument is that the collected samples are taken with constant angular spacing from the viewpoint of the scanner. This, however, does not correspond to constant spacing in the scene. Although these assumptions simplify implementation [e.g. when creating a DEM or Digital Surface Model (DSM)], the resulting models are of poor quality. Additionally, such models cannot support perfectly vertical surfaces. Without overlapping samples, an infinite slope would be required to represent vertical surfaces.

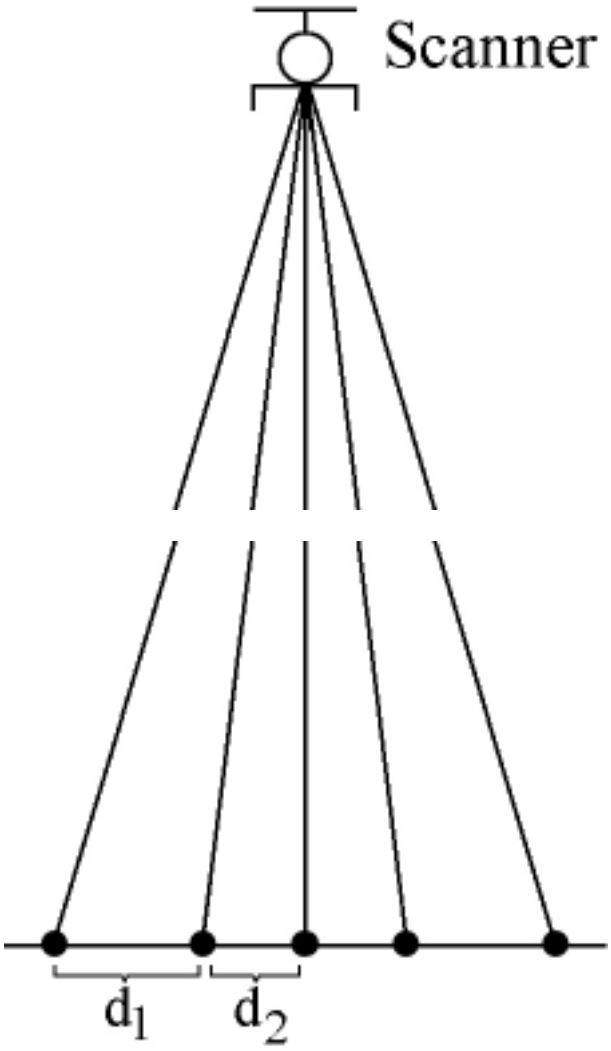

Fig. 6. Laser pulses are emitted at regular angular intervals from the scanner. However, the spacing between the point samples (dots) on the ground is not regular (i.e. $d_2 > d_1$).

Sithole and Vosselman [30] noted that ALS data are inherently irregular spaced. This fact is important, because typically, point data are sampled in some sort of regular grids (e.g. regular pixels or voxels), but that paper (like the techniques previously discussed) ignores the possibility that point samples can overlap in the vertical direction. The technique assumes that there is only one height value associated with every patch on the ground. That assumption reduces the dimensionality of the data set from 3D to two-and-a-half dimension (2.5D) and like the height thresholding approach discards significant amounts of the data.

TOWARDS AUTOMATED BUILDING EXTRACTION

The most recent work in the field of building extraction from raw laser data, which are semi-automatic or automatic methods, can be divided into two major categories as either model-driven or data-driven [31]. The first technique tries to fit certain shapes to the data. The model-driven approaches are more robust in the presence of noise and are often simple from a computational point of view, but are limited by the fact that shapes have to be given as input, and therefore require a certain amount of a priori knowledge about building shapes. As such, Haala et al. [31] proposed four different house primitives and their combinations to derive automatically 3D building geometry from ALS and existing ground planes of buildings. Texture was taken from terrestrially-based photographs [32]. You et al. [33] generated building models by adapting a set of appropriate geometric primitives and fitting strategies. Although the algorithm was able to model a variety of complex buildings with irregular shapes, it required user interaction, and these models

lack both overall detail and building wall details. Further, Hu et al. [34] used a combination of linear and non-linear fitting primitives to reconstruct a complex building. Aerial imagery was aided to refine models and improve accuracy. These techniques all neglect building wall details. In the most extreme case, walls are simply extruded from the ground-plane employing user-selected or computed building outlines. In contrast, the second technique tries to extract shapes directly from the given data set. The data-driven approaches are capable of modeling arbitrary building shape and do not need a priori knowledge as in the model-driven approaches, but they are more sensitive to noise and require careful segmentation of the point samples. For highly regular structures (e.g. standalone houses in a residential development), this is not a problem, but in more organic and/or historic areas this is not simple. A common approach is to cluster points on building roofs and then determine roof planes. Building walls are then simply extruded up to the roof height along the building outline, to produce box-like buildings with detailed roofs. As such, Vosselman and Dijkman [35] used a Hough transform for extraction of plane faces (roof planes) from the ALS data, and then 3D building models were reconstructed by combining ground planes and detected roof planes. An example of this is also covered in patent WO2006121457 [36], which used the fitting of primitives (planes and prisms) to build a 3D surface model from a point cloud. The workflow is presented as 3D building reconstruction but does not seem to include segmentation or post-processing of the raw point data; therefore assuming it to be done already.

In an attempt at reconstruction of detailed geometric building façades from LiDAR data, elevation points of the building façade were considered. In 2001, Morgan and Habib [37] were the first to consider point samples on the building façades. They used simulated data sets because at the time, ALS technology was not thought capable of acquiring sufficient vertical surface data. In that approach, no segmentation method was proposed. Even as late as 2004, Vosselman et al. [38] provided a survey paper on structure detection in raw point clouds that assumed no vertical overlap. On one level, the assumption is easy to understand as the point density vertically can only be a fraction of that collected horizontally and with a traditional single-pass flight plan oriented parallel to the streets vertical data density would be relatively sparse. Using newly devised, overlapped, flight paths oriented diagonally to the street grid has increased significantly vertical data density of the building façades, as schematically shown in Fig. 7. However, providing sufficient sampling density of vertical surfaces for reconstructing high details of the building facades still remains a challenging issue. In following paragraphs, recent efforts at extraction of building outlines and reconstruction of roof shapes for building models from common data sources such as aerial stereo images or LiDAR data or both are briefly described.

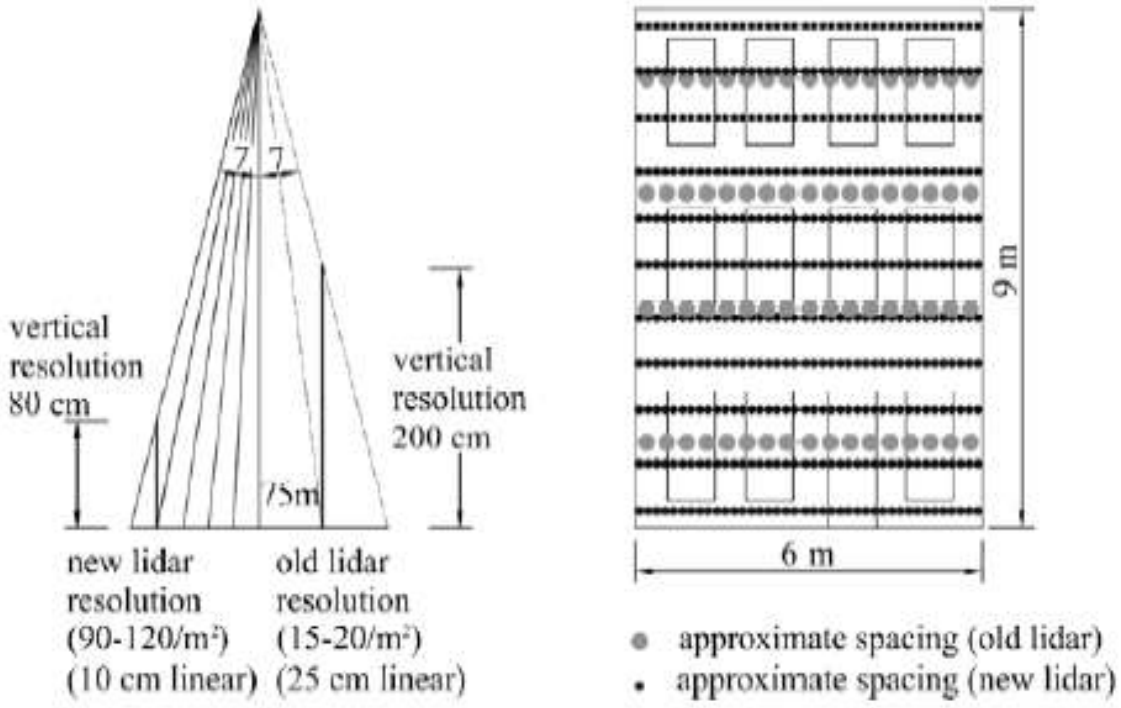

Fig. 7. Resulting vertical point density from new diagonally-oriented, overlapped, aerial flight path based on [1]

For extracting building outlines, in patent KR20030032626 [39], quadratic function curves are fitted on scan lines in a 3D image (height field), which is based on an initial 2D projection of the data, and the curvature difference between these curves is thresholded in the segmentation step. Also, patent US7515153 [40] presented a method to extract a building polygon shape from a wide aerial image, which is to generate a map efficiently. From at least one position in a building existing within an aerial photograph, a polygon of a building region is extracted based on a result of discriminating a colour around the given position. The roof texture analysis is conducted by determining sample colour for matching pixels for detection of the building region. Then, a polygon line and a vector of the polygon line of the building region are generated. Similarly, in patent US7733342 [41], there is a method of extracting building height and location through shadow analysis from a single aerial image of a building, using time and date of capture, area of capture, and camera location. The azimuth and altitude angles of the camera are initially calculated. A building roof is manually located. A height value is assigned to the extracted contour of the building roof and adjusted until the location of the shadow projected onto the image coordinates based on the assigned height coincides with the location of the actual shadow of the building existing on the image. The building's geometry is then extracted by translating the extracted contour of the building roof using the height value and vertical line of the building. Additionally, Vallet et al. [42] presented an algorithm to enhance building footprint detection by splitting the footprints along their principal directions and remerging them to make subsequent 3D reconstructions easier, more accurate and more robust. The algorithm is based on a segmentation energy that incorporates the horizontal and vertical gradients of raster data (photos or DEM).

The potential richness of such previously discarded data slowly begins to emerge in 2003 with patent JP20031346144 [43], in which a building area is extracted from laser data provided by aerial laser radiation. An image is created from the laser data through orthogonal projection. Then, a simple depth image is used for edge extraction. An alternative approach divides the scan points into grid data, in which the grid size was adopted between one to two times the raw data point spacing [44]. The cell value is set to be the median of 8-neighbour cells, if the grid cell is treated as having no data, and the 8 neighbours are classified as "non-empty". Then, the region growing based on a height difference from the central pixel is applied. The technique was devised to identify terrain, building, or vegetation based on their geometric and topology descriptions. Similarly, Dorninger and Nothegger [45] offered a new segmentation algorithm inspired by a grid-based approach. It is based on a Euclidean metric, as opposed to Delaunay triangulation, but assumes that 2D boundary polygons are known for each building. Additionally, Kabolizade et al. [46] applied a height threshold to a DSM in order to extract man-made and natural objects with different heights over a terrain. After removing trees from the DSM data, building edges were detected from the DSM by a Canny edge detection operator. These parameters of a snake model were optimised by a genetic algorithm to improve extraction of building boundaries. The results generated better compliance with the true building contours, reduced operator involvement, and improved overall speed. Alternatively, based on the decision level fusion of textural and spatial information extracted from LiDAR range and intensity data, Samadzadegan et al. [47] proposed a multi-agent methodology for building and tree recognition. Two different operational levels based on the types of contextual information are employed. First, both object-recognition agents decide on the types of objects in the study area based on textural information to generate the candidates of the building and tree region. In the second operational level, building and tree recognition agents perform some operations at the macro-level to modify the candidate building and tree regions based on spatial information. The proposed method still needs further agent definition and contextual information for the recognition process but incorporates different source information to enhance the potential capabilities.

In the most recent patents, a manual process [48] is proposed to generate topographical models of man-made structures from raw point cloud data based upon a peak histogram of height values of data points within a selected building area, or the centre of the first or predominant height cluster that meets a predetermined set of statistical criteria. Users select building shapes based upon a trade off between visual resemblance and acceptable error for each building, which depends upon the particular error parameters for a given geospatial model dataset. Then, a topological building is replaced by data within the user-selected building area based upon the building shape and height. Also, for identifying buildings from ALS data, Matei et al. [49] classified point cloud data into ground and non-ground points representing buildings and clutter, in which non-ground points were those that were higher than a predetermined threshold. The processing segmentation included four steps: estimating local surfels (local planar patches) of the non-ground points, grouping non-ground surfels into coarse regions by using a bottom-up region growing technique, fitting points to the plane by employing an expectation maximization technique, and segmenting building regions from the planes. Contours of each building segment were extracted by using a ball-pivoting algorithm [50].

Although point cloud density has increased significantly in recent years, it is not generally sufficient for reconstructing building models because of various architectural styles among urban and rural regions. In efforts to reconstruct geo-

metric building models, a common approach is to reconstruct a building's roof, and then generate a primitive of the building's roof and the building outline by using various sources as LiDAR data or aerial image. Patent JP 2003141567 [51] presented an algorithm to generate a 3D city model from detection of roof edge lines (such as gables). A boundary edge between a building and a ground was detected based on a range data with 3D coordinate values of the surface shape. The plane of the roof of the building was divided, and a polygon of outlier roof edges of each building was detected from roof edges formed between the adjoining areas. The 3D model was generated from the polygon of the roof edges. In WO 2008/094301 [52], a multi-direction gradient calculation was introduced to identify types of building roofs from building roof data points, in which the building roofs are assumed to be flat, sloped, domed, or complex. Each building's data points were divided into multiple grids, and then the sum of the distance of opposite sides of the grid was calculated. Data points of each building roof were extracted based upon an aggregation of localized peak data points. The standard deviation of the elevation histogram data was compared to a threshold, in order to identify each building's roof type. Also, Kim and Shan [53] modeled building roofs from ALS data. Roof segmentation was simultaneously determined multiple segmentations by the method of multiphase and multichannel level sets. The local planarity of each ALS point was analyzed, and normal vectors of planar points were used for segmentation, which was done by applying two level set functions to segment up to four directional planes. Then, coplanar and parallel planes are further separated into individual roof segmentation through analyzing their connectivity and homogeneity. Consequently, roof structure points were determined by intersecting adjacent roof segments and connected based on their topological relations inferred from the segmentation outcome. Although the proposed approach can reconstruct multiple roof segmentations and more complex roofs, the method requires the separation of building points from others, and sufficient data points representing roof segmentations, depends on the average data point density of the input data.

To combine LiDAR data and optical imaging data, patent TW252910B [54] extracted the 3D structure lines of the building based on mutual data exchange obtained by merging the two data sources above. Alternatively using ALS data and existing ground plans, Kada and McKinley [55] decomposed building footprints into sets of non-intersecting cells. Points inside a cell were then compared to a library of template roof shapes. Roof shapes were then determined from the normal directions of the ALS points. The validity of this approach was tested as part of 3D city models of East Berlin and of Cologne. As the decomposition of a ground plan has numerous cells, a roof may be comprised of many cells, which causes difficulty in fitting a parametric roof plane. Alternatively, patent GB2457215 [56] proposed using a plane fitting algorithm from fusing airborne optical data with ALS range data or DSMs with conditions of the roof slope and minimum size for building detection. In this technique, an initial building footprint was generated by individual, orthogonal, or linear segments and then the refined building outline was achieved using filtered stereo matched points with a least-squares' estimation. The building's roof was constructed by implementing a least-squares' plane fitting, for which the building outline, the minimum size of the planes, and the maximum height tolerance between adjacent points were the restricted conditions. Subsequently, neighbouring planes were merged using Boolean operations for generation of solid features. Elshehaby and Taha [57] presented three approaches based on a maximum likelihood classification by combining spectral satellite images and ALS data for building detection. The first approach is based on classification of multispectral satellite image, while the height information from ALS data is combined to a spectral channel in the second approach. The third approach is based on classification of a normalized difference vegetation index from multispectral satellite image and height information from ALS data as additional channels, in which the building is detected by application of a predefined value of the normalized difference vegetation index based on its histogram and of a different height threshold to normalized digital surface model (DSM). The last approach proved superior for building detection, as well as for separation of buildings from trees, when compared to first two approaches. Those building detection efforts were subsequently improved by using a "knowledge engineer" (including hypotheses, rules and conditions for identify buildings) that is available in ERDAS Imagine 8.7 software. Furthermore, by combining ALS data and multi-spectral aerial images, change detection of buildings in earlier 3D building models was introduced in 20100150431 [58]. In that, a height threshold was selected to identify ground areas, while vegetation areas were determined from the spectrums of red light and infrared light in the aerial image for non-occluded areas and from a texture image of the normalized digital surface model through classification likelihood. Ground and vegetation areas were eliminated from ALS point clouds, and then wall points, which were the lowest points of vertical triangles generated by triangulated irregular network (TIN), were also removed. Plane equations of building roofs were obtained by calculating coordinates of the building corners. Then, height distance between roofs and the laser scanning point clouds were calculated. Characteristics of the change types can be determined by change areas and change ratios in the roof plane compared to a threshold, measured as a ratio of changed points to total points or as a ratio of changed points to total point density.

Additionally, readers can refer to Haala and Kada [59] for a historical overview of building reconstruction approaches

over the last two decades. Unfortunately none of the methods exploits the full richness of the ALS dataset both with respect to variation patterns in the vertical data distribution (as seen in Fig. 7) or with respect to flight path data. As described below, a recently filed patent PTO 56793223 [60] attempts to do both with a series of discrimination functions.

ROBUST AUTOMATED BUILDING OUTLINE EXTRACTION

Airborne laser scanning produces point samples represented as (x, y, z)-tuples in a 3D space. The x- and y-coordinates can be regarded as a point sample's horizontal position, and the z-component as height. For urban areas, it is not uncommon for the number of point samples in the hundreds of millions per square kilometer. The point samples represent distances from the scanner to objects in the underlying scene. The scanner's position is known at all times and, therefore, the point samples can be considered as related to each other. Since an infinite number of point samples are required to represent even a single object completely, objects in the scene are represented incompletely.

Although working with surfaces is usually preferable to point samples, reconstructing surfaces from a collection of point samples is not trivial. Most often, only permanent man-made objects (e.g. buildings and other permanent structures) are of interest in the surface reconstruction process. This means that any reconstruction method must distinguish between points that are sampled on man-made objects and natural objects. To this end, being able to identify building walls is a first step towards making this distinction. When viewed from above, building walls appear as lines and are, therefore, herein referred to as building outlines. Building outlines represent the geographic boundaries of the data. Building surface reconstruction is then based only on the points with the boundaries of the building's outlines. For this reason, building outline detection is an important step in surface reconstruction.

An overview of this method is shown in . 8. What distinguishes this from previous methods is its complete independence from a priori knowledge. The procedure involves mapping to a 2D grid herein referred to as binning, followed by the generation of an intensity image based on a discrimination function, and the subsequent application of a Hough transform from which parametric lines can be established automatically.

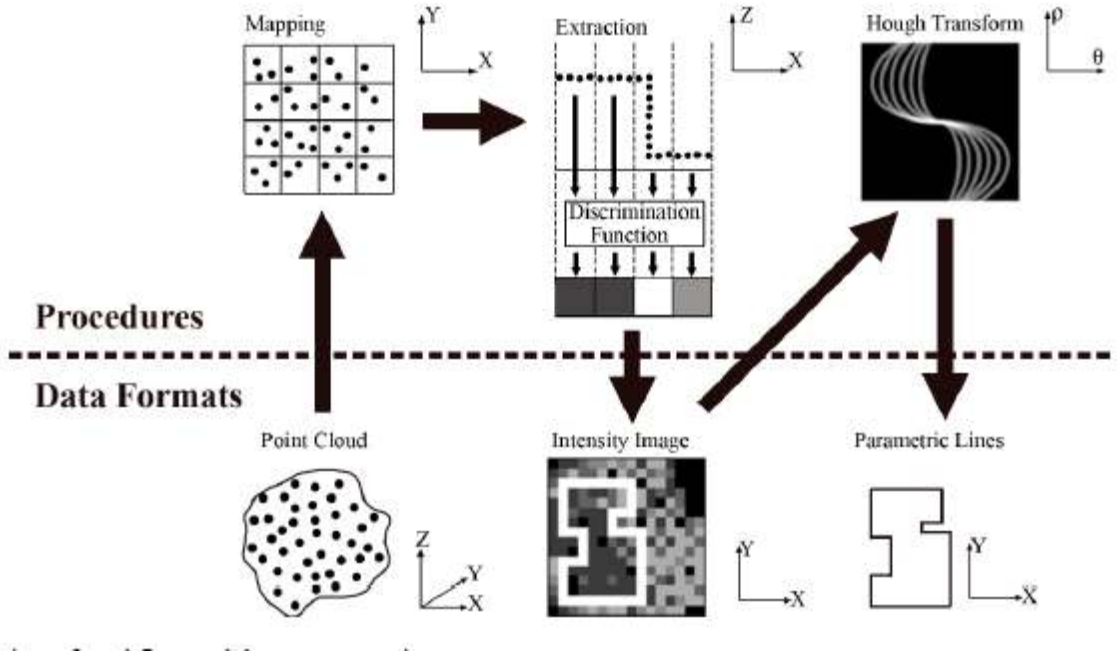

Fig. 8. An overview of workflow and data representations.

The first processing step involves mapping all the point samples onto pixels (Fig. 9). The next step involves image processing, which assumes an image (i.e. a grid of pixels laid out in a regular square pattern). The data must therefore be converted to an image. This is conventionally done by observing that each pixel corresponds to a square region on the ground, which therefore becomes a bin for collecting observations. Each pixel is then assigned one or more values

representing summary information about all points that fall into the corresponding bin. Hinks et al. [60] arrange a model of the image plane to cover the entire horizontal extent of the point clouds. The mapping subdivides the point cloud into smaller groups of points. The grouping is based on the *x*- and *y*-coordinates of the points. Points are mapped onto the same pixel belong to the same group. The pixel size must be selected with respect to the level of detail on objects represented by the point clouds. If the point clouds are sparse and pixel resolution is high, many pixels will have no or only a few points mapped onto them. Optimally, pixel groups contain enough points to allow subsequent stages of processing to robustly identify vertical surfaces. Presently, it has yet to be determined exactly how many points are required per pixel and how much this number will vary depending upon different point distributions. Therefore, pixel resolution should be an input parameter in this method.

Next, a scalar value is computed for each pixel using a discrimination function. This function requires only a set of points as its input; no external data (e.g. building ground plans) are required. The discrimination function is designed to assign bright values to those pixels, which are mapped from the points of the building walls. For each pixel, the discrimination function is applied to the mapped points, and the resulting value is assigned to the pixel. These pixels, each with a scalar value, become an intensity image and reconsider the data's presentation in 2D. Additionally, the unneeded data (e.g. vegetation) can be deemphasized by assigning low intensities to the pixels, which are mapped from the points without indicating the presence of vertical surfaces. The idea can be exemplified with a simplified case. Consider a pixel that has ten points mapped to it, and all of these ten points are close to ground level, with the simplistic assumption that ground level is the plane in 3D space where the z-component equals zero. Therefore, it is unlikely that these points were sampled on a vertical surface, since one of the characteristics of points sampled on a vertical surface is that they are distributed in the vertical direction, and not in the horizontal plane. Thus, a low intensity is assigned to the pixel.

The final step in transforming the intensity image to a set of building outlines is accomplished by applying a Hough transform [61] to the pixels in the intensity image. A Hough transform works by taking each pixel and transforming the location of the pixel within the image and its intensity to a so-called parameter space. Within this space, the equations describing the lines present in the intensity image can be extracted. The sample data set is a part of a larger data set of 6 km^2 captured during a 2007 flyover of Dublin, Ireland's cite center. The subset used for initial testing is a 250 m by 250 m area.

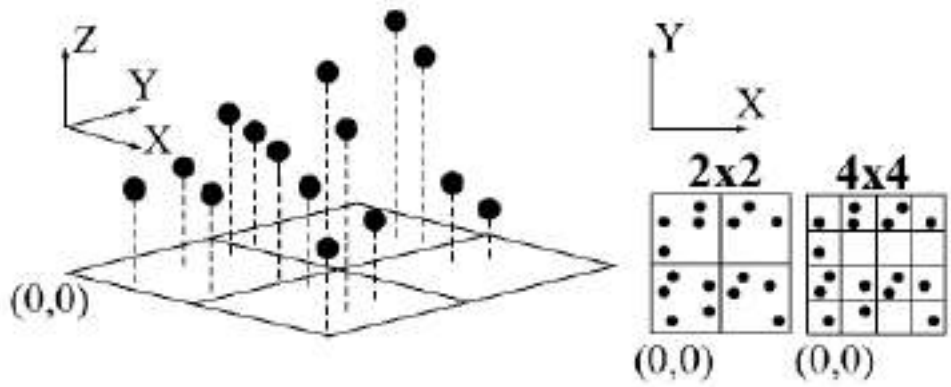

Fig. 9. Left: Perspective view of a collection of point samples in relation to the image plane onto which they are mapped. Points are mapped according to their *x*- and *y*-coordinates. Right: Top view showing two different pixel resolutions. Note that higher resolution leads to smaller pixels and, thus, less points per pixel.

The technique is robust and flexible as it uses few parameters, which rely only on intrinsic geometric features present in the data, and can be adapted to a wide range of urban geometries, as will be further explained below. The method does not require users to optimize a large number of non-intuitive parameters, while still allowing users to customize functions rather than choosing scalar parameters (e.g. threshold values). Furthermore, the method is not limited by occlusions that arise when working with aerial orthophotos. This means building outlines that are occluded when viewed directly from above are still detectable. For instance, some buildings have overhanging roof parts that occlude the fa-

çade when viewed from above (Fig. 10). The method [60] can detect these cases, despite overhanging obstructions. Additionally, the method [60] employs a discrimination function that is customizable and can exploit flight plan data, as well as data distribution within each pixel. Thus, this provides a new way of reasoning during the segmentation of the large point clouds. Thus, the input provided to the Hough transform is a new kind of intensity image, which depends not only on the minimum and the maximum values, but also on the values computed from a set of points and, thus, incorporating inter-relational properties not found in single points. Further, the usage of the first order properties, such as a normal, is avoided since such values are often not available. Finally, computing a normal is also avoided as it would require checking points in neighboring pixels for nearest neighbors, and thus rely on the relationship between pixels and the rotation angle of the image plane (although [60] is not completely rotationally invariant). To look for vertical surfaces in the specific pixels makes more sense than checking for changes between neighboring pixels, which requires searching for implicit characteristics of vertical surfaces in these pixels. Further, this technique [60] facilitates the future application of complex adaptive subdivision schemes.

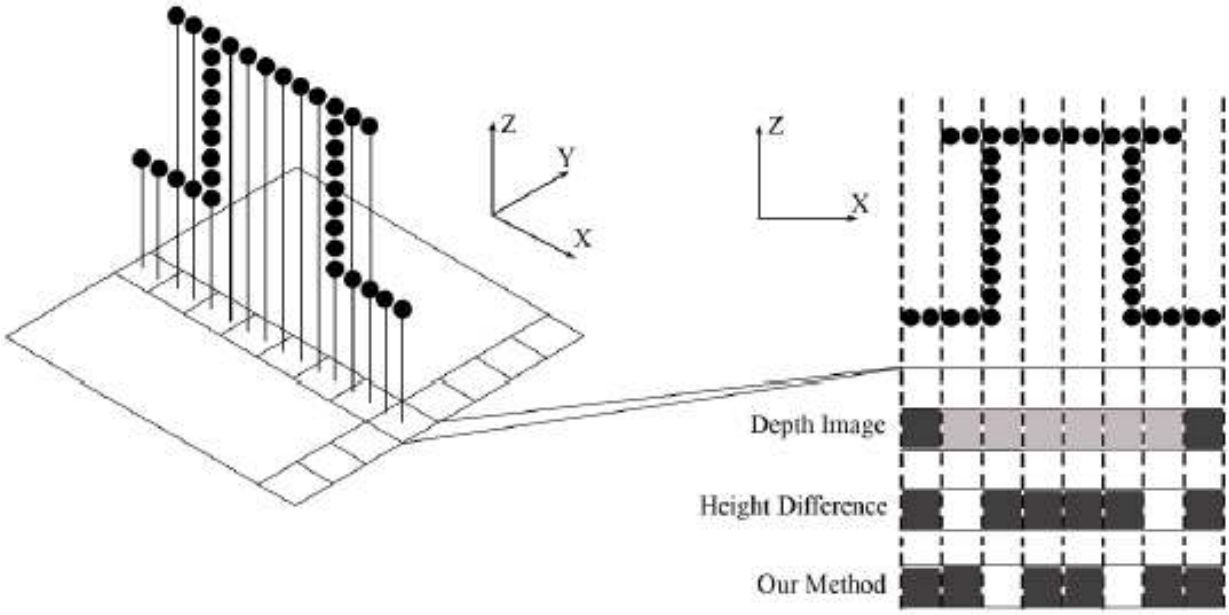

Fig. 10. Left: A section of a building shown in relation to the image plane. Right: Height differencing segmentation methods erroneously identify building walls at incorrect locations from depth images for buildings with overhanging roof parts. Using [60] avoids this problem.

Implemented in C++, using either LAS or ASCII data for its input file, the inclusion of flight path information allows prediction of the expected number of point samples within a pixel. This allows a more robust use of the number of points within each pixel in future discrimination functions. In Fig. 11, application of the method clearly shows building outlines as brighter than their surroundings. Also, the false outlines that emerged in Fig. 4 by application of a simple height threshold have now disappeared by using the discrimination function in Equation 1.

$$f_D(n, \Delta z) = \frac{n e^{(\Delta z / \Delta z_{max})}}{n_{max}}$$

[Equation 1]

where n is the number of points mapped to the pixel, Δz the height difference between the lowest and the highest points in the pixel (not across the entire dataset), n_{max} the maximum number of points found in any pixel, and Δz_{max} the largest height difference found in any pixel (Fig. 12). In this case, the discrimination function depends only on the point count and height difference – properties exclusively of the mapped points.

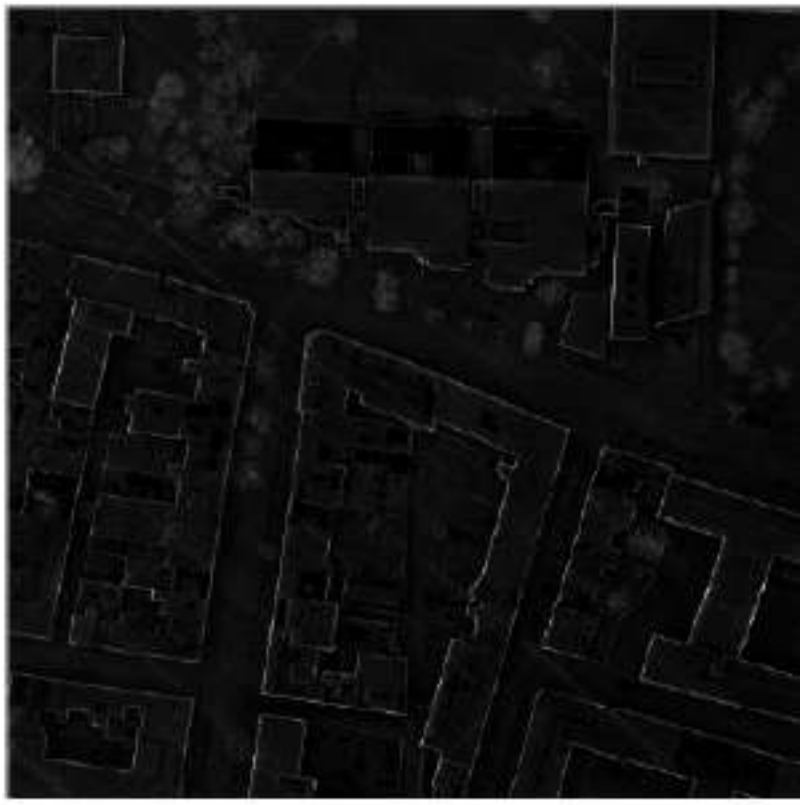

Fig. 11. Building outlines (identified by using the discrimination function with the full 3D nature of the point clouds. The pixel size represents an area of *0.25* m^2, and the image dimensions are *500* by *500* pixels).

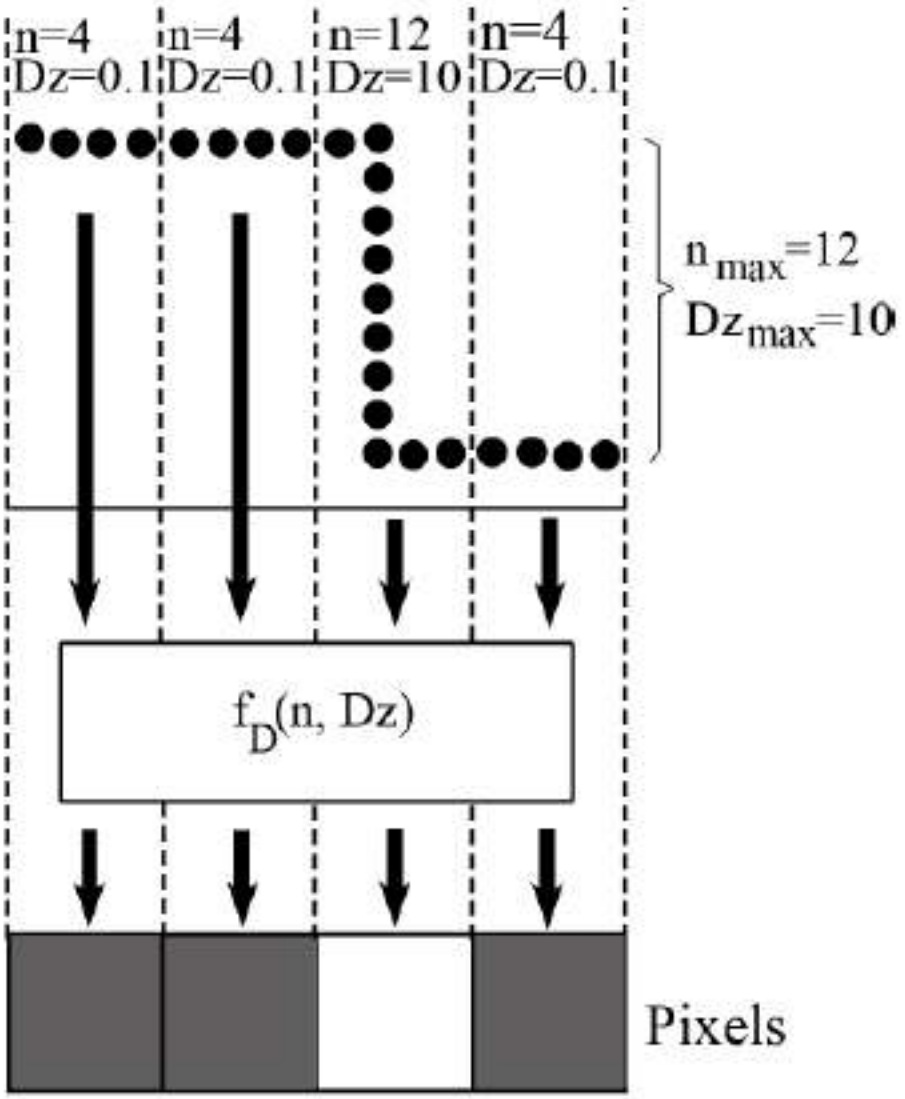

Fig. 12. Illustration of the input parameters of the displayed discrimination function $f_D(n, \Delta z)$ takes into account only the number of points per pixel, n, and the height difference between the lowest and highest point in each pixel, Δz.

The discrimination function assigns larger intensities to pixels with large point counts and large height differences. By assigning the height difference as an exponential term, its importance is enhanced. The main reason for this is that the spatial irregularity of the point samples makes the point count a less robust measure. This problem arises directly beneath the scanner, where the point density is high, without a substantial presence of vertical surfaces. Off to the sides, point density decreases on horizontal surfaces, but the presence of a vertical surface will again increase the point density. Consequently, a large point count can be either a horizontal patch directly beneath the scanner, or a vertical surface, making the point count a somewhat ambiguous measure.

CURRENT AND FUTURE DEVELOPMENTS

Since segmentation according to [60] can be used for an arbitrary image plane, it is theoretically possible to detect any planar features present in the data by aligning the plane correspondingly (Fig. 13). To do so, the characteristics of the extracted surfaces must be generalized. Extracting vertical surfaces is then a special case of this more general formulation that occurs when the image plane normal is parallel to the z-axis (i.e. the image plane is horizontal). For instance, to find all the planes in the point clouds with a 45° orientation to the ground, the image plane can be oriented accord-

ingly to extract roof planes. The point distribution within the bins would vary drastically as the image plane orientation changes.

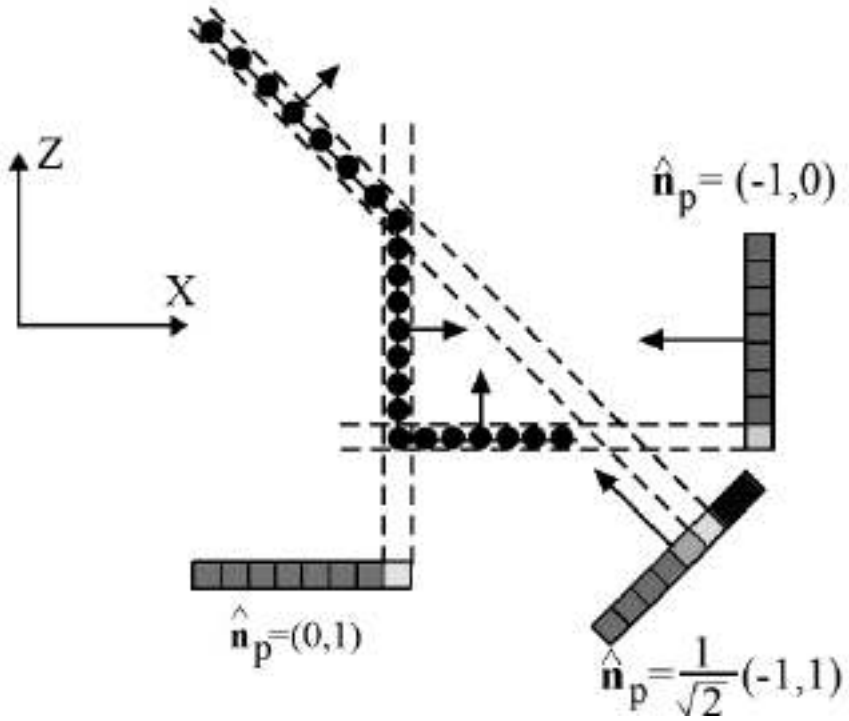

Fig. 13. This 2D example illustrates how the image plane orientation can be varied in order to extract non-vertical planes. Each image plane has an associated normal $\hat{n}_\pi$, which describes the plane's orientation. Further, each image plane has a highlighted pixel that indicates that the point distribution in this pixel is likely to be a surface of interest. Using vector notation, this reasoning can be extended to 3D.

Although recent research efforts were successful in reconstruction of building models in a large-scale city, they are mostly semi-automatic, which requires user operations and knowledge of building information. These algorithms have not yet been implemented into commercial software to generate 3D models of the city and require interactive tasks depending upon the complexity and detail level required of the city model 3D model. Development of fully automatic algorithms is still considered a research topic.

Requirements for high levels of details in 3D model city from LiDAR data is a growing challenge, because current point densities do not sufficiently represent the wide range of architectural styles of existing building facades. Current sample point density roughly reconstructs roof shapes but not building outlines [62] as they were often generated from roof edges, which may or may not reflect the buildings' outlines. The use of a ground plane or combining aerial images improves building outline detection, but adds complexity while failing to exploit the latent information of the geometric distribution of the point clouds. Mathematical theories to improve flight path planning and better incorporate flight related parameters [1] will continue to improve inputs. However, large occlusions make use of mobile laser scanner (MLS), which is terrestrially based and is a potential cost- and time-effective tool for collecting data of the vertical walls. Combining MLS and ALS data should offer new approaches for reconstructing 3D city models with high levels of architectural detail [63,64].

LIST OF ABBREVIATIONS

Airborne Laser Scanner: ALS
Computer Aided Design: CAD
Digital Elevation Model: DEM
Digital Surface Model: DSM

Geographic Information Systems: GISs
Global Positioning System: GPS
Light Detection and Ranging: LiDAR
Mobile Laser Scanner: MLS
Three-Dimensional: 3D
Triangulated Irregular Network: TIN
Two-Dimensional: 2D
Two-and-a-Half Dimensions: 2.5D

ACKNOWLEDGMENTS

This work was generously supported by Ireland's Science Foundation grant 05/PICA/I830 "GUILD: Generating Urban Infrastructures from LIDAR Data".

REFERENCES:

[1]. Hinks T, Carr H, Laefer DF. Flight Optimization Algorithms for Aerial LiDAR Capture for Urban Infrastructure Model Generation. Journal of Computing in Civil Engineering, ASCE 2009; 23(4): 330-9.

[2]. Laefer DF, Pradhan AR. Evacuation Route Selection Based on Tree-Based Hazards Using Light Detection and Ranging and GIS. Journal of Transportation Engineering, ASCE 2006; 132(4): 312-20.

[3]. Radke J, Cova T, Sheridan MF, Troy A, Mu L, Johnson R. Challenges for GIS in Emergency Preparedness and Response. ESRI White Paper; Available at: http://www.esri.com/library/whitepapers/pdfs/challenges.pdf (Access on: Mar 20, 2011)

[4]. Kevany MJ. GIS in the World Trade Center Attack - trial by fire. Computers, environment and urban Systems 2003; 27(6): 571-83.

[5]. Haile AT. Integrating Hydrodynamic Models and High Resolution (DEM) LIDAR for Flood Modelling. MSc thesis. International Institute for Geo-informational Science and Earth Observation, Enschede, The Netherlands.

[6]. Veldkamp JG, Bremmer CN, Hack HRGK, Hendriks MAN, Kronieger R, Ozmutlu S, et al. Combination of 3D-GIS and FEM modelling of the 2nd Heinenoord Tunnel, the Netherlands. *International Symposium EngGeolCity – 2001 'Engineering Geological Problems of Urban Areas.* Ekaterinburg, Russia, July 30t-August 2, 2001.

[7]. Popescu V, Hoffmann C, Kilic S, Sozen M, Meador S. Producing High-Quality Visualizations of Large-Scale Simulations. *Proceedings of the 14th IEEE Visualization 2003 (VIS'03).* Seattle, Washington, USA, October 19-24, 2003; 575-80.

[8]. Zwicker M, Gotsman C. Meshing Point Clouds Using Spherical Parameterization. *Eurographics Symposium on Point-Based Graphics.* ETH Zurich, Switzerland, June 2-4, 2004; 173-80.

[9]. Jepson W, Liggett R, Friedman S. Virtual modelling of urban environments. Presence 1996; 5(1): 83-95.

[10]. Hamill J, O'Sullivan C. Virtual Dublin: A Framework for Real-Time Urban Simulation. Journal of WSCG 2003; 11: 221-5.

[11]. Debevec PE, Taylor CJ, Malik J. Modeling and Rendering Architecture from Photographs: A Hybrid Geometry- and Image-Based Approach. *Proceedings of the 23rd annual conference on Computer graphics and interactive techniques.* New orleans, LA, USA, August 4-9, 1996.

[12]. Teller S. MIT City Scanning Project: Fully Automated Model Acquisition in Urban Areas; Available at: http://city.lcs.mit.edu/city.html (Access on: March 20, 2011)

[13]. Coorg SR. Pose Imagery and Automated Three-Dimensional Modeling of Urban Environments. PhD thesis. Massachusetts Institute of Technology, Cambridge, USA, 1998.

[14]. Wang X, Totaro S, Taill F, Hanson A, Teller S. Recovering Facade Texture and Microstructure from Real-World Images. *Proceeding 2 nd International Workshop on Texture Analysis and Synthesis at ECCV.* 381-6.

[15]. Lee SC, Jung SK, Nevatia R. Automatic Integration of Façade Textures into 3D Building Models with A Projective Geometry Based Line Clustering. Computer Graphics Forum 2002; 21(3): 677-86.

[16]. Parish YIH, Müller P. Procedural Modeling of Cities. *Proceedings of the 28th annual conference on Computer graphics and interactive techniques.* Los Angeles, CA, USA, August 12-17, 2001; 301-8.

[17]. Sun J, Yu X, Baciu G, Green M. Template-Based Generation of Road Networks for Virtual City Modeling. *Proceedings of the ACM symposium on Virtual Reality Software and Technology.* Hong Kong, China, Novermber 11-13, 2002; 33-40.

[18]. Yap CK, Biermann H, Hertzman ALC, Meyer J, Pao HK, Paxia T. A Different Manhattan Project: Automatic Statistical Model Generation. *SPIE Conference on Visualization and Data Analysis.* San Jose Convention Center, San Jose, California, USA, January 20-25, 2002; 259-68.

[19]. Wonka P, Wimmer M, Sillion F, Ribarsky W. Instant Architecture. ACM Transactions on Graphics 2003; 22(3): 669-77.

[20]. Laycock RG, Day AM. Automatically Generating Large Urban Environments Based on The Footprint Data of Buildings. *Proceedings of the Eighth ACM Symposium on Solid Modeling and Applications.* Seattle, Washington, USA, June 16-20, 2003; 346-51.

[21]. Dikiaiakou M, Efthymiou A, Chrysanthou Y. Modeling the Walled City of Nicosia. In: 4th Int'l Symp. Virtual Reality, Archaeology and Intelligent Cultural Heritage, 2003 November 5-7, 2003 Brighton, United Kingdom.

[22]. van Veen HA, Distler HC, Distler HK, Braun SJ, Bülthoff HH. Navigating Through A Virtual City: Using Virtual Reality Technology to Study Human Action and Perception. Future Generation Computer Systems 1998; 14(3-4): 231-42.

[23]. Sony Computer Entertainment Europe. The Getaway. London; 2002.

[24]. Hinks T. Geometric Processing Techniques for Urban Aerial Laser Scan Data. PhD thesis. University College Dublin, Dublin, Ireland, January, 2011.

[25]. Vosselman G, Dijkman E. 3D Building Model Reconstruction from Point Clouds and Ground Plans. ISPRS International Archives of Photogrammetry and Remote Sensing 2001; 34(3/W4): 37-43.

[26]. Chen L, Teo T, Rau J, Liu J, Hsu W. Building Reconstruction from LiDAR Data and Aerial Imagery. *Proceedings of the IEEE International Geoscience and Remote Sensing Symposium.* Seoul, Korea, July 25-29, 2005; 2846-9.

[27]. Novacheva A. Building Roof Reconstruction from LiDAR Data and Aerial Images Through Plane Extraction and Colour Edge Detection. ISPRS International Archives of the Photogrammetry, Remote Sensing and Spatial Information Sciences 2008; 37(Part B6b): 53-7.

[28]. Hofmann P. Detecting Urban Features from IKONOS Data Using an Object-Oriented Approach. *Proceedings RSPS 2001.* London, UK, September 12-14, 2001; 79-91.

[29]. Hofmann AD, Maas HG, Streilein A. Knowledge-Based Building Detection Based on Laser Scanner Data and Topographic Map Information. *Photogrammetric Computer Vision, ISPRS Commission III, Symposium 2002.* Graz, Austria, September 9 - 13, 2002; 169-74.

[30]. Sithole G, Vosselman G. Automatic Structure Detection in A Point-cloud of An Urban Landscape. *2nd GRSS/ISPRS Joint Workshop on Remote Sensing and Data Fusion over Urban Areas.* Technical University of Berlin, Berlin, Germany, 22-23 May 2003; 67-71.

[31]. Dorninger P, Pfeifer N. A Comprehensive Automated 3D Approach for Building Extraction, Reconstruction, and Regularization from Airborne Laser Scanning Point Clouds. Sensors 2008; 8(11): 7323-43.

[32]. Haala N, Brenner C, Anders Kh. 3D Urban GIS From Laser Altimeter And 2D Map Data. International Archives of Photogrammetry & Remote Sensing 1998; 32(3): 339-46.

[33]. You S, Hu J, Neumann U, Fox P. Urban Site Modeling from LiDAR. *Proceedings of the 2003 international conference on Computational science and its applications.* Montreal, Canada, May 18-21, 2003; 579-88.

[34]. Hu J, You S, Neumann U, Park KK. Building Modeling from LiDAR and Aerial Imagery. *ASPRS 2004.* Denver, Colorado, USA, May 23-28, 2004; 1-6.

[35]. Vosselman G, Dijkman S. 3D Building Model Reconstruction from Point Clouds and Ground Planes. *International Archives of Photogrammetry and Remote Sensing.* Annapolis, MA, USA, October 22-24,2001; 37-43.

[36]. Verma V, Hsu SC. Method and Apparatus for Performing Three-dimensional Computer Modelling. Patent WO/2006/121457, 2006.

[37]. Morgan M, Habib A. 3D TIN Automatic Building Extraction from Airborne Laser Scanning Data. *ASPRS Annual meeting, Gateway to The New Millenium.* St. Louis, MO, USA, April 23-27, 2001; CD ROOM.

[38]. Vosselman G, Gorte BGH, Sithole G, Rabbani T. Recognising Structure in Laser-Scanner Point Clouds. ISPRS International Archives Photogrammetry, Remote Sensing and Spatial Information. Sciences 2004; XXXVI(8/W2): 33-8.

[39]. Chul LJ. Device and Method for Detecting Edge in 3D Image. Patent KR20030032626, 2003.

[40]. Jin H, Iwamura K, Ishimaru N, Hino T, Kagawa Y. Map Generation Device, Map Delivery Method, and Map Generation Program. Patent US7515153, 2009.

[41]. Kim T. Method of Extracting 3D Building Information Using Shadow Analysis. Patent US7733342, 2010.

[42]. Vallet B, Pierrot-Deseilligny M, Boldo D. Building Footprint Database Improvement for 3D Reconstruction: A Direction Aware Split and Merge Approach. *CMRT09, IAPRS.* Paris, France, September 3-4, 2009; 139-44.

[43]. Masaomi O. Method and System for Extracting Outline of Building. Patent JP2003346144, 2003.

[44]. Forlani G, Nardinocchi C. Adaptive Filtering of Aerial Laser Scanning Data. *Proceedings of the ISPRS Workshop 'Laser Scanning 2007 and SilviLaser.* Espoo, Finland, September 12-14, 2007; 130-5.

[45]. Dorninger P, Nothegger C. 3D Segmentation of Unstructured Point Clouds for Building Modelling. *PIA07-Photogrammetric Image Analysic.* Munich, Germany, September 19-21, 2007; 191-6.

[46]. Kabolizade M, Ebadi H, Ahmadi S. An Improved Snake Model for Automatic Extraction of Buildings from Urban Aerial Images and LiDAR Data. Computers, Environment and Urban Systems 2010; 34(5): 435-41.

[47]. Samadzadegan F, Mahmoudi FT, Schenk T. An Agent-Based Method for Automatic Building Recognition from LiDAR Data. Canadian Journal of Remote Sensing 2010; 36(3): 211-23.

[48]. Patrick K, Mark R, Stephen C, Harlan Y. Geospatial Modeling System Providing Building Generation Based Upon User Input on 3d Model And Related Methods. Patent WO2009045843, 2009.

[49]. Matei BCM, Samarasekera S, Kim JY, Karney CFF, Sawhney HS, Kumar R. Building Segmentation for Densely Built Urban Regions Using Aerial LiDAR Data. Patent Patent US2009310867, 2009.

[50]. Bernardini F, Mittleman J, Rushmeier H. The Ball-Pivoting Algorithm for Surface Reconstruction. IEEE Transactions on Visualization and Computer Graphics 1999; 5(4): 349-59.

[51]. Madhavan B, Saika O, Kazuhiko Y. Three-dimensional City Model Generating Device and method of Generating Three-Dimensional City Model. Patent JP2003141567, 2003.

[52]. Rahmes M, Yates H, Connetti S, Smith AOn. Geospatial Modelling System Providing Building Roof Type Identification Features and Related Methods. Patent WO/2008/094301, 2008.

[53]. Kim KH, Shan J. Building Roof Modeling from Airborne Laser Scanning Data Based on Level Set Approach. ISPRS Journal of Photogrammetry and Remote Sensing 2011; In Press, Corrected Proof.

[54]. Jian CL, Jian-You R, Jin-Jin L, Guo-Shin S, S W-C. Extract Method for 3-Dimensional Structure Lines of Building. Patent TW252910B, 2006.

[55]. Kadaa M, McKinley L. 3d Building Reconstruction from Lidar Based on A Cell Decomposition Approach. *CMRT09. IAPRS.* Paris, France, September 3-4, 2009; 47-52.

[56]. Nikolaos K. Automatic 3D Modelling. Patent GB2457215, 2009.

[57]. Elshehaby AR, Taha LG. A New Expert System Module for Building Detection in Urban Areas Using Spectral Information and LIDAR Data. Applied Geomatics 2009; 1(4): 97-110.

[58]. Chen L-c, Huang C-y, Teo T-a. Method of Change Detection for Building Models. Patent US 20100150431, 2010.

[59]. Haala N, Kada M. An Update on Automatic 3D Building Reconstruction. ISPRS Journal of Photogrammetry and Remote Sensing 2010; 65(6): 570-80.

[60]. Hinks T, Carr H, Laefer DF, Morvan Y, O'Sullivan C, Truong-Hong L, et al. Robust Building Outline Extraction. Patent PTO 56793223 2009.

[61]. Hough PVC. Method and means for recognizing complex patterns. Patent US3069654, 1962.

[62]. Elberink SO, Vosselmana G. Quality Analysis on 3D Building Models Reconstructed from Airborne Laser Scanning Data ISPRS Journal of Photogrammetry and Remote Sensing 2011; 66(2): 157-65.

[63]. Jochem A, Höfle B, Rutzinger M. Extraction of Vertical Walls from Mobile Laser Scanning Data for Solar Potential Assessment. Remote Sensing 2011; 3: 650-67.

[64]. Rutzinger M, Elberink SO, Pu S, Vosselman G. Automatic Extraction of Vertical Walls from Mobile and Airborne Laser Scanning Data. *ISPRS Workshop Laser Scanning 2009*. Paris, France, September 1-2, 2009; 7-11.